MMSL
Military Medical
Science Letters

Mil. Med. Sci. Lett. (Voj. Zdrav. Listy) 2013, vol. 82(3), p. 102-114
ISSN 0372-7025
DOI: 10.31482/mmsl.2013.015

## ORIGINAL ARTICLE

# MODELING THE BINDING OF CWAs TO AChE AND BuChE

**Brian J. Bennion[1], Edmond Y. Lau[1], Jean-Luc Fattebert[2], Patrick Huang[3], Eric Schwegler[3], William Corning[4], Felice C. Lightstone[1]✉**

[1] Biosciences and Biotechnology Division, Mailstop L-372, Lawrence Livermore National Laboratory, 7000 East Ave, Livermore CA, 94550.
[2] Computation Directorate Mailstop L-561, Lawrence Livermore National Laboratory, 7000 East Ave Livermore CA 94550.
[3] Condensed Matter and Materials Division, Mailstop L-198, Lawrence Livermore National Laboratory, 7000 East Ave Livermore CA 94550.
[4] Deer Valley High School, 4700 Lone Tree Way, Antioch, CA 94531

Received 10th February 2013.
Revised 25th March 2013.
Published 6th September 2013.

**Summary**

Traditional chemical weapon agents (CWAs) are known to bind acetylcholinesterase (AChE) and butyrylcholinesterase (BuChE). Their lethality is known to be different for different mammalian species. We have modeled the binding affinity of CWAs to AChE and BuChE in human, rabbit, rat and mouse using molecular docking and free energy calculations. Through molecular docking we are able to correctly bind the CWAs at the active site. Using molecular mechanics generalized Born surface area (MMGBSA) calculations, we determined the binding free energy in the active site. Through these calculations, we observe that correct orientation at the active site is critical to binding.

*Key words: AChE; BuChE; computational docking; molecular dynamics simulations; binding free energy calculations*

## INTRODUCTION

Acetylcholinesterase (E.C. 3.1.1.7) (AChE) and butyrylcholinesterase (E.C. 3.1.1.8) (BuChE) are members of the alpha/beta hydrolase superfamily and are inhibited by organophosphate (OP) compounds. Acetylcholine is a potent neurotransmitter in both the central nervous system (CNS) and the peripheral nervous system (PNS). AChE is critical for the termination of acetylcholine signaling in the synapse, and inactivation of AChE by OP compounds causes a buildup of acetylcholine, leading to flooding of the nicotinic acetylcholine receptor. Unchecked acetylcholine can lead to a massive disturbance in the cholinergic system, respiratory arrest, and death [1, 2]. Many studies [3-8] have been published in order to understand how AChE enhances the rate of hydrolysis of acetylcholine $10^{12}$ times relative to the aqueous reaction [9].

Each AChE active site is composed of a catalytic triad (Ser203, Glu334, and His447 according to the human sequence numbering) that sits at the bottom

✉ Lawrence Livermore National Laboratory, Mailstop L-372, Biosciences and Biotechnology Division, 7000 East Ave, Livermore CA 94550, USA
lightstone1@llnl.gov

of a narrow ~20 Å deep gorge (see Figure 1). Just at the mouth of the gorge is the peripheral anionic binding site (PAS) (Trp286, Tyr72, Tyr124, Glu285, Asp74 and Tyr341) (see Figure 1). The active site is composed of two parts, the esteratic and choline sub-sites, for binding the carboxyl and the positively charged choline end of acetylcholine, respectively (see Figure 1). The reaction mechanism, which can be separated into the acylation and deacylation steps, has been described previously [3, 10, 11] and is shown in Scheme 1.

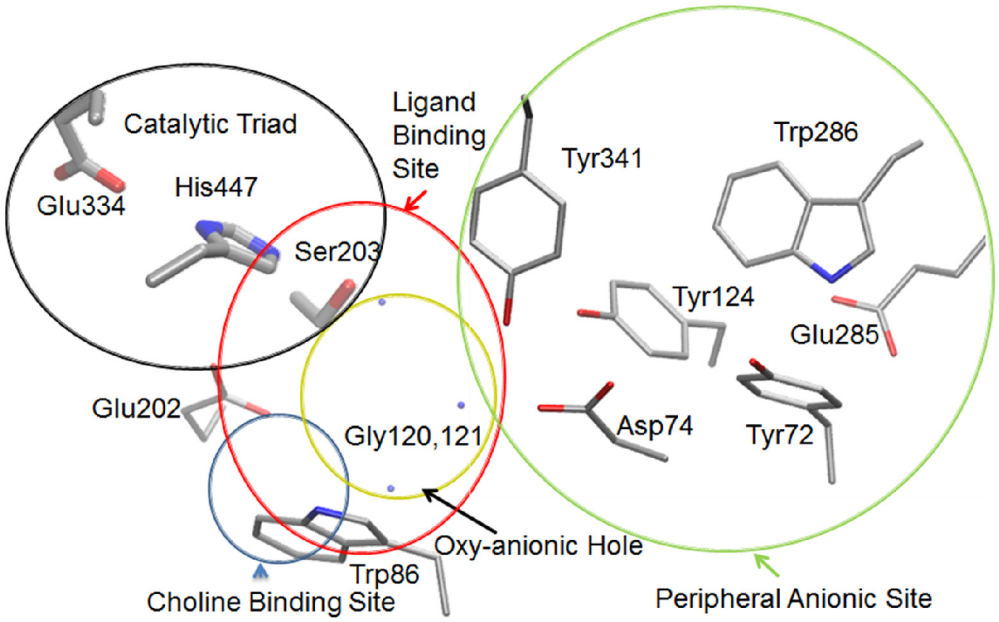


**Figure 1:** The active site structural topology of human AChE (PDBID:1B41). The catalytic triad lies at the end of the narrow but deep 20 A gorge. The PAS residues are located at the beginning of the gorge and may function as gate keepers. The choline binding site is defined mostly by Trp86. The oxy-anionic hole in black holds the carbonyl oxygen in place with the backbone amide hydrogens of Gly120, 121 and Ala204 shown as blue dots. Preservation of this sub-site is critical for maintaining a catalytically competent binding conformation. Figure made with VMD [57] and rendered with Tachyon [58].

**Scheme 1:**

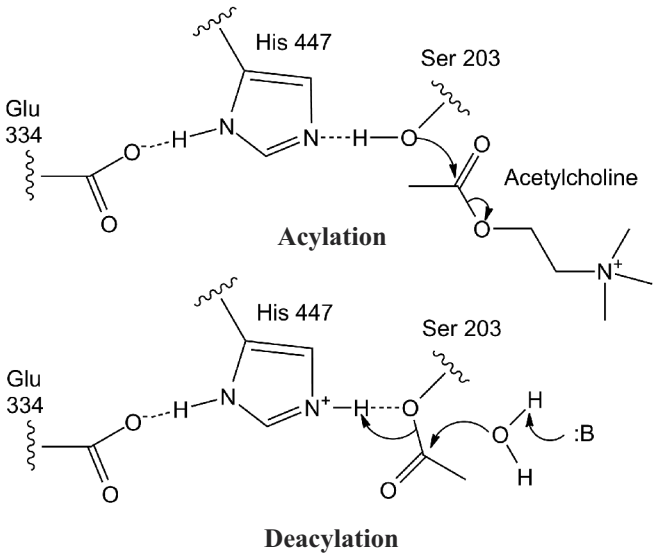

Butyrylcholinesterase was discovered more than 80 years ago [12] and is found throughout the body [13]. BuChE catalyzes the hydrolysis of numerous esters of choline. Although AChE is the primary enzyme for the hydrolysis of acetylcholine, BuChE is a putative backup enzyme for that reaction [14]. While the reason for BuChE's widespread presence in the body is not well understood [15], some postulate its purpose was originally as a toxin scavenger of natural poisons including solanidine, physostigmine, cocaine, and other naturally occurring toxins [16]. BuChE had garnered relatively little attention until the military realized pretreatment with BuChE could confer limited temporal protection to OP nerve toxins, such as tabun, soman, sarin, and VX, by acting as a sponge for these compounds, thus protecting the cholinergic system [17, 18]. BuChE detoxifies by covalent bonding with the OP, stoichiometrically, and shows no adverse effect to an organism when bound.

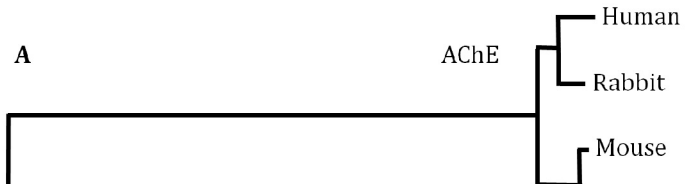


| Enzyme | Oxyanionic Site | Anionic Site | PAS | Aryl Site |
|---|---|---|---|---|
| Ache | | | | |
| Mouse | AGG | EA | YDYEWY | FFF |
| Rat | AGG | EA | YDYEWY | FFF |
| Rabbit | AGG | EA | YDYEWY | FFF |
| Human | AGG | EA | YDYEWY | FFF |
| BuChE | | | | |
| Mouse | AGG | EY | NDQERY | LIF |
| Rat | AGG | EY | NDQEKY | RIF |
| Rabbit | AGG | EY | NDQEVY | LVF |
| Human | AGG | EY | NDQEAY | LVF |

**Figure 2:** AChE and BuChE evolved at significantly different times. In general, human and rabbit enzymes are more related to each other than to mouse or rat (A). Sequence indentity between enzyme families for each species is between 51-53%. Species within each family have a sequence identity that is greater than 80%. Significant differences exist between AChE and BuChE in the peripheral anionic site, where aromatic residues have been replaced with ionizable residues in the BuChE sequence (B). Variation is also observed in the Anionic and Aryl Sites. Phylogenic analysis was perfomed using COBALT from the NCBI [59].

As shown in Figures 1 and 2, the homology between the different species is very high for both enzymes. The active site in the four AChE proteins is identical out to a radius of 10 A. At this point conservative changes are present at position 294 and 336. Val294 in human is replaced with isoleucine in the rodent AChE proteins and is just below the entrance of the gorge. Ser336 is replaced by threonine in the rabbit protein. These and other changes in sequence may influence the dynamics of the protein and therefore catalysis.

The intra and interspecies sequence differences between BuChE are significant. BuChE from some species have the capacity to self-rehabilitate certain OP inhibited enzymes [15, 19]. In human BuChE, there are over 65 genetic variants that exhibit differing degrees of inhibition in the phenotype and catabolize of drugs and poisons [20] [21-26]. Understanding the properties of BuChE variants has important implications for human response to OP pesticides and nerve agents and to the efficacy of post exposure treatment [27].

To address the variability in CWA toxicity between commonly used rodent models and humans, close examination of the enzyme targets from the various species are performed. For the current work,

we make the simple assumption that the majority of the toxicity of CWAs is contributed by the binding and reaction with AChE and BuChE. We compare the binding of CWAs to both AChE and BuChE. Computational docking and binding free energy calculations for four species (human, rabbit, rat, and mouse), four traditional chemical agents (VX, tabun, soman and sarin), and two natural substrates (acetylcholine and butyrylcholine) are presented, and the results further illuminate the interspecies differences.

## METHODS

### *Homology Modeling*

AChE and BuChE enzyme homology models were created using the Modeller program [28, 29]. For AChE, the mouse structure (PDBID: 1N5M) was used as the template for the creation of the rat, rabbit, and human structures. BuChE homology models for rat, rabbit, and mouse were based on the human (PDBID:1XLW) structure. Initially, ten homology models were created for each protein from each species. Generally, three disulfide bonds were present in the models (except mouse BuChE). The catalytic HIS residues for all enzymes were kept neutral.

### *Molecular Docking*

Docking simulations of traditional CWAs (sarin, soman, VX, and tabun) and substrates (acetylcholine or butyrylcholine) to AChE and BuChE were performed with Autodock (version 3.0.5) [30] or Autodock Vina [31]. The different enzyme models and ligands were prepared for docking using Autodock Tools [32]. A united atom representation was used for both the ligands and enzyme. Charges for the ligands were obtained from AM1-BCC calculations using the program Antechamber. The bonds in the ligands were set to be rotatable to maximize the flexibility of the ligand. Grid boxes were centered at the oxygen of the catalytic serine and varied in size from 16 Å to 28 Å depending on the size of the ligand.

### *Molecular Dynamics Simulations*

The best pose for each species enzyme/ligand co-complex was selected for energy minimization and molecular dynamics simulations. The $P_S$ enantiomer was used for all CWA based simulations [33, 34] (see Scheme 2).

**Scheme 2:**

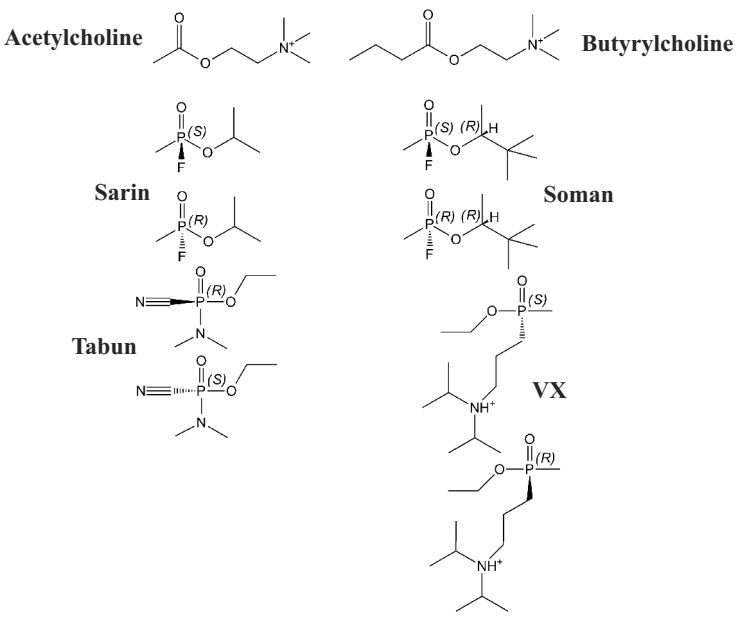


All molecular dynamics (MD) simulations were performed using the program NAMD (version 2.6) [35] using the CHARMM27 force field [36]. The holoenzyme was solvated in a box of water [37] with a minimum of 10 Å of water between the enzyme and the edge of the box. The water boxes varied from 75 Å to 94 Å on a side. Counter ions ($Na^+$ and $Cl^-$) were added to neutralize the charge

of the system and to bring the salt concentration to 0.15 M. The final system contained ~8000 enzyme atoms and ~15000 total atoms. The system was subjected to several hundred steps of steepest descent minimization. Restrained MD simulations were performed at 310 K using the NPT ensemble with periodic boundaries. A Langevin piston was used to control the pressure, and a Nose-Hoover thermostat kept the temperature constant at 310 K. Electrostatic interactions were calculated using particle mesh Ewald summation (PME) methods. Short-range interactions were cutoff at 9 Å. The SHAKE algorithm was used and allowed a timestep of 2 fs. Equilibration of the systems was performed in five steps of restrained dynamics with all heavy atoms initially restrained with a force constant of 40 kcal/mole•Å$^2$. The final constraint of 1 kcal/mole•Å$^2$ was necessary to keep the ligands in catalytically competent conformations. Each MD simulation was performed for 10 nanoseconds with snapshots being saved every 1 ps.

*MM-GBSA Calculations*

More accurate binding energies were calculated using the molecular mechanics-generalized born/solvent accessible surface area protocol as described by Habtemariam et al. [38]. The electrostatic contribution to the solvation free energy was calculated using the Generalized-Born molecular volume (GBMV) [39, 40] method within CHARMM (version 31b1) [41]. The non-polar contribution to the solvation free energy was calculated using the equation $E_{np} = \gamma SA$ where $\gamma$ = 7.2 cal/Å$^2$, and SA is the solvent accessible surface area using a probe radius of 1.4 Å. Each calculation included 500 snapshots from the MD simulations.

## RESULTS AND DISCUSSION

Standard molecular docking, MD simulations and MMGBSA calculations of AChE, BuChE, and CWAs bound within the active site of AChE and BuChE are presented. To evaluate the difference in binding of CWAs between species of AChE or BuChE and to compare the binding of the same CWA between AChE and BuChE, a well-defined catalytically competent ligand pose was necessary. Given that AChE is an extremely well-studied enzyme, the catalytic and surrounding residues are well known. The mechanism as shown in Scheme 1, has the serine oxygen attacking the carbonyl carbon. In the case of the CWAs, the electrophile is the phosphorus atom. The assumed mechanism for the CWAs is that the serine oxygen will attack the phosphorus atom in an in-line formation, where the leaving group is 180° from the serine oxygen. For all the CWAs, the serine should be within 4 Å of the phosphorus atom. In the case of sarin and soman, the leaving group is $F^-$. In the case of VX the leaving group is diisopropylaminoethanethiol (DESH). The tabun leaving group is $CN^-$. From previous studies, the phosphonyl oxygen needs to be bound in the oxyanion hole, which is defined by Gly120, Gly122 and Ala204 amide hydrogen atoms. Distances between the amide hydrogen atoms and the phosphonyl oxygen should be <2.5 Å. On the other side of the gorge is the choline binding site, which is defined by a tryptophan (Trp 86/82). The catalytically competent pose should have the aliphatic tails of each ligand interacting through non-polar interactions with Trp 86/82 (see figure 1). The docking results below support the use of these criteria.

*Molecular Docking*

The docking energies for the six ligands docked with eight enzymes correlate with size of the ligand in the case of AChE and to a limited extent in BuChE (see Table 1). The reported energies are for the $P_S$ enantiomer of the CWA. Many studies have shown that the $P_S$ enantiomer is a better substrate than $P_R$ for AChE [33, 34, 42] (see Scheme 2). Because the natural substrate is acetylcholine, we can only assume an in-line attack mechanism and have made this assumption for the mechanism of the CWAs as well. However, a recent QM/MM study has shown that an adjacent attack is a favorable mechanism for tabun [43], reinforcing the idea that other mechanisms should be probed. We chose poses from the docking with these stereochemical and non-bonded interactions in mind even though the observed docking value may not have been the most favorable.

In general, VX is calculated to be the strongest binding CWA to AChE, which is consistent with experimentally determined lethality [44-46]. In rat and mouse AChE, acetylcholine is a stronger binder than VX. Interestingly, in the case of rabbit and human, VX binds stronger than acetylcholine, the natural substrate. From experimental studies, VX is observed to be more lethal to rabbits and humans than rats and mice [47]. In all species of AChE, sarin was the weakest binder, and tabun and soman had

**Table 1.** Docked energies (in kcal/mole) and inhibiton constants ($M^{-1}*min^{-1}$) for ligands in AChE and BuChE.

| AChE | Tabun | Sarin | Soman | VX | Acetylcholine | Butyrylcholine |
|---|---|---|---|---|---|---|
| **Rat** | -5.43 | -4.53 | -5.71 | -6.07 | -6.12 | ND |
| **Mouse** | -5.18 | -4.95 | -5.90 | -6.59 | -6.83 | ND |
| **Rabbit** | -5.57 | -4.47 | -5.38 | -7.45 | -5.87 | ND |
| **Human** | -5.61 | -4.58 | -5.38 | -7.05 | -5.96 | ND |
| **Human ($k_i$)** | 3.0 x $10^{6}$ [c] | 3.2 x $10^{7}$ [a] | 9.2 x $10^{7}$ [a] | 1.4 x $10^{8}$ [b] | | |
| **BuChE** | | | | | | |
| **Rat** [d] | -5.90 | -4.80 | -5.80 | -4.1 | -3.20 | -5.70 |
| **Mouse** | -4.36 | -3.87 | -4.26 | -5.08 | -5.02 | -6.40 |
| **Rabbit** | -4.43 | -3.82 | -4.24 | -4.80 | -4.93 | -6.83 |
| **Human** | -3.99 | -3.93 | -4.46 | -4.71 | -5.16 | -6.19 |
| **Human ($k_i$)** | 2.0 x $10^{6}$ [c] | 3.2 x $10^{7}$ [a] | 2.8 x $10^{8}$ [a] | 1.1 x $10^{7}$ [e] | | |

[a] [44] [b] [45] [c] [46] [d] Rat docking energies were calculated from Autodock VINA [31]. [e] [48]

similar binding energies. Because sarin and tabun are the smallest agents and form the fewest number of contacts with the enzyme, these two CWAs, not surprisingly, are the weaker binders. Comparison of inhibition constants for human AChE shows the calculated docking data is reasonable and in the correct order. VX is the strongest inhibitor followed by soman, sarin, and finally tabun.

The docked conformations of the CWA and acetylcholine are similar in all the species of AChE in this study. There are 3 important interaction sites for any ligand within the protein: the oxyanion hole, the hydrophobic pocket near the catalytic triad (Trp236, Phe295, Phe297, and Phe338), and Trp86. To have a conformation that was catalytically competent, the oxo-group of the CWA and the carbonyl oxygen of acetylcholine had to be in contact with the oxyanion hole. Hydrogen bonds where formed between the backbone amides of Gly120, Gly121, and to some extent Ala204 with the oxo-group. All of these CWAs have a small hydrophobic moiety (in many cases a methyl group) coming off the phosphorous that is directed

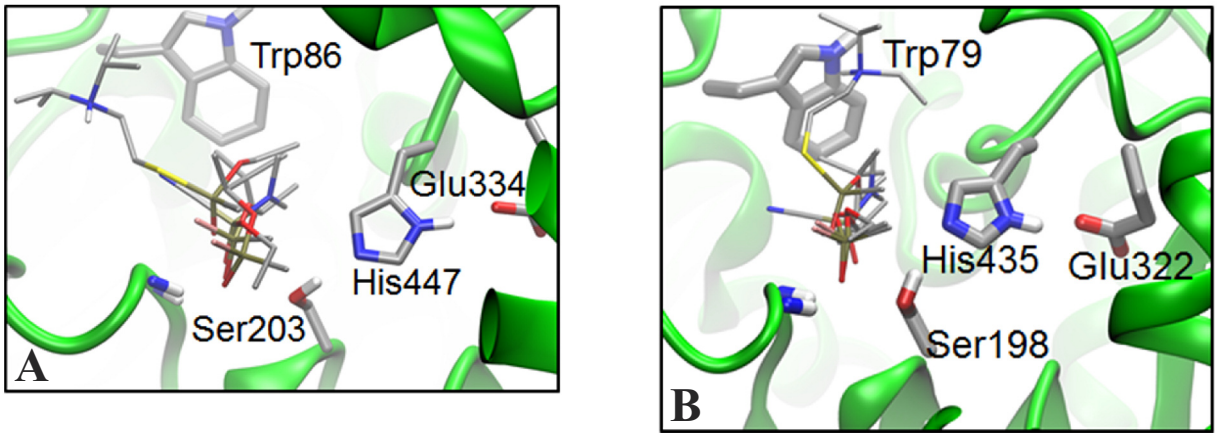


**Figure 3.** Docked conformations of sarin, tabun, and VX, in the active site of human AChE (A). BuChE (B) also shows acetylcholine and butyrylcholine docked to the active site. The larger gorge is visible to the left of the ligands in B. In addition, there is a larger space in the acyl binding pocket which is bounded by Ile283 in BuChE. None of docked poses displayed were predicted to be the most energetically favorable. However, these poses did make the appropriate hydrogen bonds and contacts that define a catalytically active conformation. Figures made with VMD [57] and rendered with Tachyon [58].

towards the hydrophobic group by the catalytic triad. Additionally, a larger moiety attached to the phosphorous is directed towards Trp86. Acetylcholine has its quaternary ammonium group positioned to interact with the indole group of Trp86. The pi-cation interaction stabilizes the ligand within the active site. Unlike the other CWAs studied, VX has a large leaving group that forms interactions with AChE. When docked, the tertiary ammonium group of the leaving group interacts with the hydroxyl group of Tyr124. An example of the docked ligand poses in AChE and BuChE is shown in Figure 3.

For BuChE, the general trend is that the larger ligands bind to all species of BuChE better than the smaller ligands. Interestingly, sarin has the best docking pose to the rat structure while the larger butyrylcholine ligand shows the best docking overall. Acetylcholine is shown to dock slightly better to the human structure than the other OP ligands. VX docks best to the mouse structure while soman shows a preference for the rat structure. Butyrylcholine docking energies in mouse and rabbit structures are slightly better than in the rat or human BuChE. In the cases of poor docking energies, there were not enough non-polar contacts with hydrophobic residues such as Trp82, Trp231, Phe329, Phe326. Additionally, electrostatic interactions were too long and obtuse angles were present in the oxyanion hole. Docking energies for tabun in both proteins values appear to be overestimated and show a significant lack of correlation with the experimental Ki value. This most likely is a result of the unusual structure of tabun. A linear cyano group coupled with the P-N bond may not be parameterized accurately in the autodock force fields. Finally, with the exception of butyrylcholine values, all BuChE docking values are less favorable than those observed in AChE. A comparison of the active site topology and representative docking poses is shown in Figures 3 and 4.

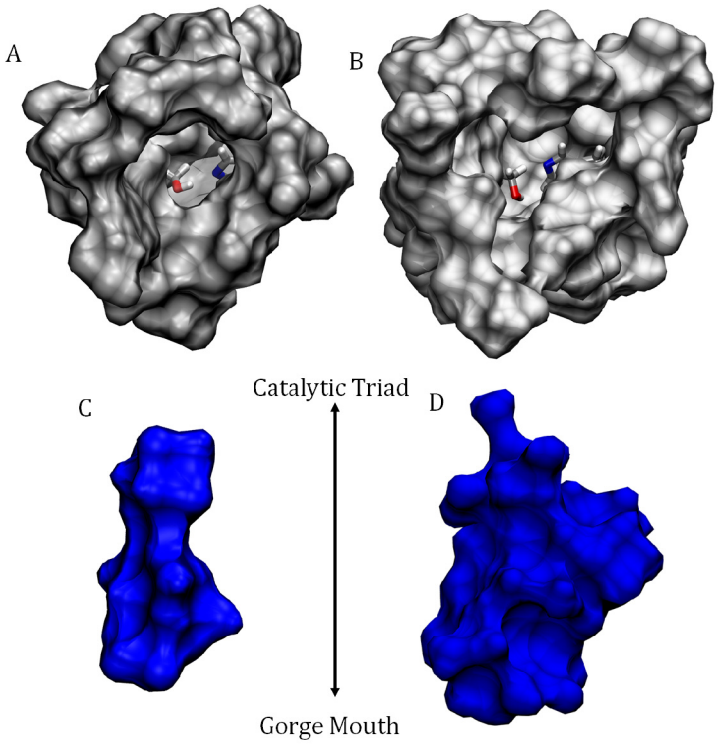


**Figure 4.** Residues comprising the gorge and active sites of AChE (A) and BuChE (B). Structures are snapshots from MD simulations and the catalytic residues are represented as licorice sticks colored by atom. Water molecules are shown in solvent surface accessible area (blue) for AChE (C) and BuChE (D). BuChE has twice the volume of AChE in the gorge and peripheral active site. The AChE gorge can hold 24 waters, at a volume of 276Å$^3$, while the BuChE gorge contains up to 47 waters, with a volume of approximately 541Å$^3$. The BuChE snapshot was taken at 1.687 ns in which a sarin molecule was initially bound in a catalytic pose. However, as the MD simulation progressed, the sarin molecule preferred to interact with members of the peripheral anionic site. Ser198 rotated to make a hydrogen bond with Ser200 amide backbone once sarin left the site. Figures are made with VDM [57] with the MSMS [60] surface algorithm and rendered with Tachyon [58]

*Structural Origins of the Differences in Docking Energies between AChE and BuChE*

In general, the docking energies are lower for all ligands in BuChE in comparison to AChE. There is one exception in that butyrylcholine docking energies are comparable to acetylcholine in AChE. Curiously, VX is a bulkier molecule than butyrylcholine, although does not dock as favorably in BuChE as in AChE. Several possibilities may explain the smaller docking values for OPs and acetylcholine in the BuChE docking calculations. Arguably, the most important factor is the large size of the BuChE active site. The volume of the BuChE gorge is twice the volume of the AChE gorge as depicted in Figure 4. The larger cavity size presents more volume for the ligand to sample. The choline binding site is farther away from the active site serine when compared to AChE. An approximation of this distance is measured between the serine and Trp82, resulting in 3-4 Å greater distance in BuChE. The larger separation accounts for the relatively larger ester based substrates that have been observed as substrates in experiments [49, 50]. However, the docking calculations are not able to compensate for the larger active site when the enzyme backbone is frozen and only important sidechains are allowed to respond to the presence of the ligand. All these factors combine to reduce the number of enzyme-ligand interactions. OP "ageing" in BuChE is uncommon, further supporting the lack of enzyme interactions when compared to AChE [48].

The docking calculations do reveal the extent to which various ligand-enzyme interactions affect the docking energy. The more favorable poses either had very strong hydrogen bonds to the oxyanion hole and short ser-OH-phosphorous distances, or there were multifaceted non-polar contacts at each end of the ligand. In all of the species of BuChE, the oxyanion interaction was modest for butyrylcholine; however the multiple hydrophobic interactions with Trp82 and Trp231 appeared to compensate. In the rabbit-tabun calculation, there were no substantial non-polar contacts observed. On the other hand, the ser-OH-phosphorous distance was the shortest yet, and there were exceptionally strong hydrogen bonds formed in the oxyanion hole. While the correlation between the docking energy and the inhibition constants were reasonable for human AChE, the correlation of docking energy to inhibition constant for human BuChE is poor. Soman is the strongest inhibitor followed by sarin, VX, and tabun.

In the case of BuChE, interspecies sequence variation might also contribute to the wide range of docking energies in the BuChE calculations. As cited earlier, the rat enzyme contains an arginine (286) residue instead of a leucine in the active site. Moreover, in the both mouse and rat structures, the human Phe395 is replaced by leucine near the esteratic site, creating a larger pocket for the aliphatic part of a ligands acyl group. The increased bulk at this position was likely responsible for the unfavorable VX results in rabbit and human BuChE since it is of comparable size to butyrylcholine.

**Table 2.** MMGBSA energies (in kcal/mole) for ligands in AChE and BuChE.

| **AChE** | **Sarin** | **Soman** | **VX** | **Acetylcholine** |
|---|---|---|---|---|
| **Rat** | ND | -9.8 (3.1) | -29.6 (1.1) | -19.9 (3.5) |
| **Mouse** | ND | -13.4 (4.6) | -29.7 (5.2) | -20.3 (1.5) |
| **Rabbit** | ND | -10.7 (5.5) | -23.2 (4.4) | -18.8 (0.6) |
| **Human** | -11.3 (2.7) | -23.8 (4.2) | -28.0 (7.7) | -18.4 (2.0) |
| **BuChE** | | | | |
| **Rat** | ND | ND | ND | ND |
| **Mouse** | ND | ND | -5.3 (4.5) | ND |
| **Rabbit** | ND | -6.2 (5.7) | -14.3 (10) | ND |
| **Human** | ND | -3.0 (0.5) | -11.8 (4.5) | ND |

ND - Values not determined due to poor statistical sampling of the ligand in the catalytically active pose in the enzyme active site. Calculations with tabun and butyrylcholine did not provide any catalytically active conformations during the molecular dynamics simulations. The reported values are the average of at least three separate GBSA calculations.

*MM-GBSA Calculations*

More accurate and technically demanding MMGBSA calculations allow for the incorporation of full enzyme/ligand motion and better treatment of solvation effects than static docking. MD simulations of ligands bound to the eight enzymes were performed to generate structural data for the MMGBSA calculations. During simulations of both AChE and BuChE, the lack of sarin-enzyme interactions for an extended time prevented a catalytically competent conformation from forming and therefore was not pursued further. Tabun simulations in both enzymes revealed similar problems and were not continued. Interestingly, this is consistent with the inhibition data that shows tabun and sarin are the weakest inhibitors. The three other ligands provide more reliable results in AChE and mixed results for BuChE.

In AChE, the native ligand acetylcholine, has calculated binding energies of about 19 kcal/mole. The largest difference between species is about 2 kcal/mole, which is consistent with the high conservation of amino acid identity in the active site of AChE. For soman and VX a difference of 5-10 kcal/mole is calculated between species. The data for soman suggest that binding to the human enzyme is preferred, while VX binds preferentially to rat and mouse. Although the energy differences between the ligands are large, the rank ordering of VX, acetylcholine, and soman appears to be reasonable.

VX is a large, positively charged molecule that forms many contacts with the enzyme. Acetylcholine is the natural substrate for AChE, and soman forms the fewest number of enzyme contacts of the ligands modeled by the MM-GBSA method. The interactions formed by soman and acetylcholine with each AChE species are similar. Three important interactions are formed between the ligands and the enzyme. The oxo-group has to interact with the oxyanion hole, the methyl group attached to phosphorous of soman and carbonyl carbon of acetylcholine are directed into the hydrophobic pocket formed by Trp236, Phe295, Phe297, and Phe338, and the pinacolyl group of soman and quaternary ammonium group of acetylcholine are directed at Trp86. VX has similar interactions with the oxyanion hole and the hydrophobic pocket, but the ethoxy group is too short to interact with the Trp86. Additionally, the large leaving group of VX tends to be extended for mouse, rat, and rabbit AChE and comes in contact with Trp86, Tyr124, and Tyr337. In the human AChE simulations, the VX leaving group interacts strongly with Trp86 and is not in an extended conformation. From the MD simulations of AChE, the most critical interaction is between the oxo-group of the ligand to the oxyanion hole of the enzyme. Once this interaction is broken, the ligand is no longer in a position to react and tends to drift away from the catalytic triad. Mutations around the oxyanion hole have shown that the disruption of this motif destabilizes the interaction between ligand and enzyme by up to 5 kcal/mole [11, 51, 52].

For BuChE, the MMGBSA calculations were extremely difficult to complete because of the same reasons as discussed previously for the docking calculations. VX and soman, which are larger and more hydrophobic ligands, provide reliable binding energies for mouse, rabbit, and human enzymes. For VX in BuChE, the binding energies are weaker than those for VX in AChE. For sarin and tabun, the required statistical sampling of the catalytic pose was not met as the ligands would drift around the active site gorge. Only by adding force-based restraints on the ligand atoms could the catalytic pose be maintained. However, the magnitude of that force restraint precluded realistic calculations of the binding energy.

*MD Simulations*

During MD simulations of both enzymes with ligands, several structural rearrangements often occur in the active site. First, the amide hydrogen of Gly120/116 in the oxyanion hole rotates 180°, effectively removing a potent hydrogen bonding partner with the ligands. We also observe significant mobility in the Glu202/197 side-chain during the simulations. The function of this residue and its protonation state has been debated. Wlodek et al stated that protonating Glu202 would decrease the acylation by 32 fold [53]. Fuxreiter and Warshel suggest little change to the acylation rate in the protonated stated [54], while Vagedes et al. suggest an enhancement of the rate in the protonated state [55]. However, Nemukhin et al show that deprotonation of Glu202 favors the acyl reaction [56]. As a result we modeled Glu202 as having a negative charge in our MD simulations. Lastly, the loop containing His447/435 tends to move and pulls the histidine away from the triad, allowing the ligand to drift and the catalytic serine to hydrogen bond with other amino acids in the enzyme.

The docking and MMGBSA simulations reveal the types and magnitude of ligand-enzyme interactions, at the atomistic scale, required for binding in catalytically competent conformations. While having a larger active site, BuChE appears to be able to provide the necessary contact points for the larger VX molecule, especially when water molecules and dynamics are added. VX binding is strongest when tight hydrogen bonds are present with Gly116-117/Ala199 amides in the oxyanion hole. Other supplementary interactions include; the ethoxy group fully interacting with Trp231, non-polar contacts between the aliphatic carbons on the charged nitrogen tail and Trp82, and a nitrogen hydrogen bond with Glu197. The slightly smaller soman compound does not contain the ethoxy group and has a less bulky and neutral pinacolyl tail. Without the added aliphatic groups, the interactions in the oxyanion hole are more susceptible to hydrogen bonds from water molecules in the active site. This competition of water molecules for the Ser203 is also observed for the ser-OH-phosphorous interaction, which upon stretching is vulnerable to being replaced by water. For smaller compounds, the competition with water for ideal enzyme interactions is much higher unless multiple ligands are bound to the enzyme.

## CONCLUSIONS

From our studies, we present the following conclusions. First, simple docking calculations can predict catalytically active poses, if the enzyme mechanism of action is known. By comparing six ligands in eight enzymes, we can also determine the fundamental ligand-enzyme interactions for binding, at least qualitatively. We find that strong hydrogen bonds in the oxyanion hole are the main determinant of favorable binding energies. We also note that many tight (<3.5 Å) non-polar contacts can compensate for a lack of strong hydrogen bonds in the oxyanion hole. These criteria appear relevant given that the human AChE binding results are in good agreement with available experimental inhibition rate constants and is worth ~5 kcal/mole. Secondly, rigorous MMGBSA calculations of the larger ligands are in agreement with data from human AChE experiments. However, this method has proven to be difficult for small ligands in both enzymes because the active site histidine is highly mobile, allowing the ligand to sample more of the active site. In addition, the BuChE active site is twice as large and structurally distinct from AChE. The active site residues in BuChE are also distinct from the same enzyme of different species. The catalytically competent pose of each compound is difficult to maintain without artificial restraints which allow for sufficient sampling. Moreover, our data suggest that other specific ligand-enzyme interactions beyond the required hydrogen bonds in the oxyanion hole are important when explicit water molecules and enzyme backbone motion are present.

## ACKNOWLEDGMENTS

We acknowledge Mrs. Alexa Malloy for her technical assistance with the manuscript. This work was supported by the Defense Threat Reduction Agency BA07TAS072 and CBS.SCIC.01.10.LLNL.004. We thank Livermore Computing for the computer time. This work was performed under the auspices of the U.S. Department of Energy by Lawrence Livermore National Laboratory under Contract DE-AC52-07NA27344. LLNL-JRNL-485260

## REFERENCES

1. Holmstedt, B., Pharmacology of organophosphorus cholinesterase inhibitors. Pharmacological Reviews, **1959**. 11(3): p. 567-688.
2. Taylor, P., Z. Radic, N.A. Hosea, S. Camp, P. Marchot, and H.A. Berman, Structural bases for the specificity of cholinesterase catalysis and inhibition. *Toxicology Letters*, **1995**. 82-3: p. 453-458.
3. Quinn, D.M., Acetylcholinesterase - Enzyme Structure, Reaction Dynamics, and Virtual Transition-States. *Chemical Reviews*, **1987**. 87(5): p. 955-979.
4. Dvir, H., I. Silman, M. Harel, T.L. Rosenberry, and J.L. Sussman, Acetylcholinesterase: From 3D structure to function. *Chemico-Biological Interactions*, **2010**. 187(1-3): p. 10-22.
5. Guo, J.X., M.M. Hurley, J.B. Wright, and G.H. Lushington, A docking score function for estimating ligand-protein interactions: Application to acetylcholinesterase inhibition. *Journal of Medicinal Chemistry*, **2004**. 47(22): p. 5492-5500.

6. Guo, J.X., J.J.Q. Wu, J.B. Wright, and G.H. Lushington, Mechanistic insight into acetylcholinesterase inhibition and acute toxicity of organophosphorus compounds: A molecular modeling study. *Chemical Research in Toxicology*, **2006**. 19(2): p. 209-216.
7. Hurley, M.M., A. Balboa, G.H. Lushington, and J.X. Guo, Interactions of organophosphorus and related compounds with cholinesterases, a theoretical study. *Chemico-Biological Interactions*, **2005**. 157: p. 321-325.
8. Lushington, G.H., J.X. Guo, and M.M. Hurley, Acetylcholinesterase: Molecular modeling with the whole toolkit. Current Topics in *Medicinal Chemistry*, **2006**. 6(1): p. 57-73.
9. Schowen, R.L., Transition states of biochemical processes, G.R. D. and R.L. Schowen, Editors. **1978**, Plenum: New Your. p. 77-114.
10. Rosenberry, T.L., Catalysis by Acetylcholinesterase - Evidence That Rate-Limiting Step for Acylation with Certain Substrates Precedes General Acid-Base Catalysis. Proceedings of the National Academy of Sciences of the United States of America, **1975**. 72(10): p. 3834-3838.
11. Zhang, Y.K., J. Kua, and J.A. McCammon, Role of the catalytic triad and oxyanion hole in acetylcholinesterase catalysis: An ab initio QM/MM study. *Journal of the American Chemical Society*, **2002**. 124(35): p. 10572-10577.
12. Stedman, E. and L.H. Easson, Choline-esterase. An enzyme present in the blood-serum of the horse. *Biochemical Journal*, **1932**. 26: p. 2056-2066.
13. Darvesh, S., D.A. Hopkins, and C. Geula, Neurobiology of butyrylcholinesterase. *Nature Reviews Neuroscience*, **2003**. 4(2): p. 131-138.
14. Barnard, E.A., Neuromuscular Transmission--enzymatic destruction of acetlycholine, in The Peripheral Nervous System, J. Hubbard, Editor. **1974**, Plenum: New York.
15. Masson, P. and O. Lockridge, Butyrylcholinesterase for protection from organophosphorus poisons: Catalytic complexities and hysteretic behavior. Archives of *Biochemistry and Biophysics*, **2010**. 494(2): p. 107-120.
16. Jbilo, O., C.F. Bartels, A. Chatonnet, J.P. Toutant, and O. Lockridge, Tissue distribution of human acetylcholinesterase and butyrylcholinesterase messenger-RNA. *Toxicon*, **1994**. 32(11): p. 1445-1457.
17. Broomfield, C.A., D.M. Maxwell, R.P. Solana, C.A. Castro, A.V. Finger, and D.E. Lenz, Protection by butyrylcholinesterase against organophosphorus poisoning in nonhuman-primates. *Journal of Pharmacology and Experimental Therapeutics*, **1991**. 259(2): p. 633-638.
18. Nachon, F., E. Carletti, M. Wandhammer, Y. Nicolet, L.M. Schopfer, P. Masson, and O. Lockridge, X-ray crystallographic snapshots of reaction intermediates in the G117H mutant of human butyrylcholinesterase, a nerve agent target engineered into a catalytic bioscavenger. *Biochemical Journal*, **2011**. 434: p. 73-82.
19. Langenberg, J.P., L.P.A. Dejong, M.F. Otto, and H.P. Benschop, Spontaneous and Oxime-Induced Reactivation of Acetylcholinesterase Inhibited by Phosphoramidates. *Archives of Toxicology*, **1988**. 62(4): p. 305-310.
20. Kovarik, Z. and V. Simeon-Rudolf, Interaction of human butyrylcholinesterase variants with bambuterol and terbutaline. *Journal of Enzyme Inhibition and Medicinal Chemistry*, **2004**. 19(2): p. 113-117.
21. Lockridge, O., genetic-variants of human serum-cholinesterase influence metabolism of the muscle-relaxant succinylcholine. *Pharmacology & Therapeutics*, **1990**. 47(1): p. 35-60.
22. Ladu, B.N., C.F. Bartels, C.P. Nogueira, A. Hajra, H. Lightstone, A. Vanderspek, and O. Lockridge, phenotypic and molecular biological analysis of human butyrylcholinesterase variants. *Clinical Biochemistry*, **1990**. 23(5): p. 423-431.
23. Mikami, L.R., S. Wieseler, R.L.R. Souza, L.M. Schopfer, F. Nachon, O. Lockridge, and E.A. Chautard-Freire-Maia, Five new naturally occurring mutations of the BCHE gene and frequencies of 12 butyrylcholinesterase alleles in a Brazilian population. *Pharmacogenetics and Genomics*, **2008**. 18(3): p. 213-218.
24. Yen, T., B.N. Nightingale, J.C. Burns, D.R. Sullivan, and P.M. Stewart, Butyrylcholinesterase (BCHE) genotyping for post-succinylcholine apnea in an Australian population. *Clinical Chemistry*, **2003**. 49(8): p. 1297-1308.
25. Flegar-Mestric, Z., B. Surina, and Z. Siftar, Biological variations of human serum butyrylcholinesterase activity in a population from Zagreb, Croatia. *Chemico-Biological Interactions*, **1999**. 120: p. 193-199.
26. Lando, G., A. Mosca, R. Bonora, F. Azzario, S. Penco, A. Marocchi, M. Panteghini, and M.C. Patrossoa, Frequency of butyrylcholinesterase gene mutations in individuals with abnormal inhibition numbers: an Italian-population study. *Pharmacogenetics*, **2003**. 13(5): p. 265-270.

27. Lockridge, O. and P. Masson, Pesticides and susceptible populations: People with butyrylcholinesterase genetic variants may be at risk. *Neurotoxicology*, **2000**. 21(1-2): p. 113-126.
28. Marti-Renom, M.A., A.C. Stuart, A. Fiser, R. Sanchez, F. Melo, and A. Sali, Comparative protein structure modeling of genes and genomes. *Annual Review of Biophysics and Biomolecular Structure*, **2000**. 29: p. 291-325.
29. Sali, A. and T.L. Blundell, Comparative Protein Modeling by Satisfaction of Spatial Restraints. *Journal of Molecular Biology*, **1993**. 234(3): p. 779-815.
30. Morris, G., D. Goodsell, R. Halliday, R. Huey, W. Hart, R. Belew, and A. Olson, Automated docking using a Lamarckian Genetic Algorithm and Empirical Binding Free Energy Function. *J. Computational Chemistry*, **1998**. 19: p. 1639-1662.
31. Trott, O. and A.J. Olson, Software News and Update AutoDock Vina: Improving the Speed and Accuracy of Docking with a New Scoring Function, Efficient Optimization, and Multithreading. *Journal of Computational Chemistry*, **2010**. 31(2): p. 455-461.
32. Morris, G.M., R. Huey, W. Lindstrom, M.F. Sanner, R.K. Belew, D.S. Goodsell, and A.J. Olson, AutoDock4 and AutoDockTools4: Automated Docking with Selective Receptor Flexibility. *Journal of Computational Chemistry*, **2009**. 30(16): p. 2785-2791.
33. Benschop, H.P. and L.P.A. Dejong, Nerve Agent Stereoisomers - Analysis, Isolation, and Toxicology. *Accounts of Chemical Research*, **1988**. 21(10): p. 368-374.
34. Benschop, H.P., C.A.G. Konings, J. Vangenderen, and L.P.A. Dejong, Isolation, anticholinesterase properties, and acute toxicity in mice of the 4 stereoisomers of the nerve agent soman. *Toxicology and Applied Pharmacology*, **1984**. 72(1): p. 61-74.
35. Phillips, J.C., R. Braun, W. Wang, J. Gumbart, E. Tajkhorshid, E. Villa, C. Chipot, R.D. Skeel, L. Kale, and K. Schulten, Scalable molecular dynamics with NAMD. *Journal of Computational Chemistry*, **2005**. 26(16): p. 1781-1802.
36. MacKerell, J., A. D., D. Bashford, M. Bellott, R.L. Dunbrack Jr., J.D. Evanseck, M.J. Field, S. Fischer, J. Gao, H. Guo, S. Ha, D. Joseph-McCarthy, L. Kuchnir, K. Kuczera, F.T.K. Lau, C. Mattos, S. Michnick, T. Ngo, D.T. Nguyen, B. Prodhom, I. Reiher, W.E., B. Roux, M. Schlenkrich, J.C. Smith, R. Stote, J. Straub, M. Watanabe, J. Wiorkiewicz-Kuczera, D. Yin, and M. Karplus, All-atom empirical potential for molecular modeling and dynamics studies of proteins. *Journal of Physical Chemistry B*, **1998**. 102: p. 3586-3616.
37. Jorgensen, W.L., J. Chandrasekhar, J.D. Madura, R.W. Impey, and M.L. Klein, Comparison of Simple Potential Functions for Simulating Liquid Water. *Journal of Chemical Physics*, **1983**. 79(2): p. 926-935.
38. Habtemariam, B., V.M. Anisimov, and A.D. MacKerell, Cooperative binding of DNA and CBF beta to the Runt domain of the CBF alpha studied via MD simulations. *Nucleic Acids Research*, **2005**. 33(13): p. 4212-4222.
39. Lee, M.S., F.R. Salsbury, and C.L. Brooks, Novel generalized Born methods. *Journal of Chemical Physics*, **2002**. 116(24): p. 10606-10614.
40. Still, W.C., A. Tempczyk, R.C. Hawley, and T. Hendrickson, Semianalytical Treatment of Solvation for Molecular Mechanics and Dynamics. *Journal of the American Chemical Society*, **1990**. 112(16): p. 6127-6129.
41. Brooks, B.R., C.L. Brooks, 3rd, A.D. Mackerell, Jr., L. Nilsson, R.J. Petrella, B. Roux, Y. Won, G. Archontis, C. Bartels, S. Boresch, A. Caflisch, L. Caves, Q. Cui, A.R. Dinner, M. Feig, S. Fischer, J. Gao, M. Hodoscek, W. Im, K. Kuczera, T. Lazaridis, J. Ma, V. Ovchinnikov, E. Paci, R.W. Pastor, C.B. Post, J.Z. Pu, M. Schaefer, B. Tidor, R.M. Venable, H.L. Woodcock, X. Wu, W. Yang, D.M. York, and M. Karplus, CHARMM: the biomolecular simulation program. *Journal of Computational Chemistry*, **2009**. 30(10): p. 1545-614.
42. Vandenberg, G.R., H.C. Beck, and H.P. Benschop, Stereochemical analysis of the nerve agents soman, sarin, tabun, and vx by proton nmr-spectroscopy with optically-active shift-reagents. *Bulletin of Environmental Contamination and Toxicology*, **1984**. 33(5): p. 505-514.
43. Kwasnieski, O., L. Verdier, M. Malacria, and E. Derat, Fixation of the Two Tabun Isomers in Acetylcholinesterase: A QM/MM Study. *Journal of Physical Chemistry B*, **2009**. 113(29): p. 10001-10007.
44. Bartling, A., F. Worek, L. Szinicz, and H. Thiermann, Enzyme-kinetic investigation of different sarin analogues reacting with human acetylcholinesterase and butyrylcholinesterase. *Toxicology*, **2007**. 233(1-3): p. 166-172.
45. Ordentlich, A., D. Barak, G. Sod-Moriah, D. Kaplan, D. Mizrahi, Y. Segall, C. Kronman, Y. Karton, A. Lazar, D. Marcus, B. Velan, and A. Shafferman, Stereoselectivity toward VX is

determined by interactions with residues of the acyl pocket as well as of the peripheral anionic site of AChE. *Biochemistry*, **2004**. 43(35): p. 11255-11265.
46. Carletti, E., H. Li, B. Li, F. Ekstrom, Y. Nicolet, M. Loiodice, E. Gillon, M.T. Froment, O. Lockridge, L.M. Schopfer, P. Masson, and F. Nachon, Aging of Cholinesterases Phosphylated by Tabun Proceeds through O-Dealkylation. *Journal of the American Chemical Society*, **2008**. 130(47): p. 16011-16020.
47. Fathimulla, F., Preliminary assessment of health impacts for the Newport Chemical Agent Disposal Facility. *Drug and Chemical Toxicology*, **2000**. 23(1): p. 55-66.
48. Wandhammer, M., E. Carletti, M. Van der Schans, E. Gillon, Y. Nicolet, P. Masson, M. Goeldner, D. Noort, and F. Nachon, Structural Study of the Complex Stereoselectivity of Human Butyrylcholinesterase for the Neurotoxic V-agents. *Journal of Biological Chemistry*, **2011**. 286(19): p. 16783-16789.
49. Yang, W.C., Y.M. Pan, L. Fang, D.Q. Gao, F. Zheng, and C.G. Zhan, Free Energy Perturbation Simulation on Transition States and High-Activity Mutants of Human Butyrylcholinesterase for (-)-Cocaine Hydrolysis. *Journal of Physical Chemistry B*, **2010**. 114(33): p. 10889-10896.
50. Canos, J., L. Andreu, R. Bolinches, F. Rogla, A. Otte, and C. Gil, Case of Succinylcholine Apnea - Identification of Genetic-Variants. *Annales De L Anesthesiologie Francaise*, **1979**. 20(2): p. 109-112.
51. Gao, D.Q. and C.G. Zhan, Modeling effects of oxyanion hole on the ester hydrolysis catalyzed by human cholinesterases. *Journal of Physical Chemistry B*, **2005**. 109(48): p. 23070-23076.
52. Ordentlich, A., D. Barak, C. Kronman, N. Ariel, Y. Segall, B. Velan, and A. Shafferman, Functional characteristics of the oxyanion hole in human acetylcholinesterase. *Journal of Biological Chemistry*, **1998**. 273(31): p. 19509-19517.
53. Wlodek, S.T., J. Antosiewicz, and J.M. Briggs, On the mechanism of acetylcholinesterase action: The electrostatically induced acceleration of the catalytic acylation step. *Journal of the American Chemical Society*, **1997**. 119(35): p. 8159-8165.
54. Fuxreiter, M. and A. Warshel, Origin of the catalytic power of acetylcholinesterase: Computer simulation studies. *Journal of the American Chemical Society*, **1998**. 120(1): p. 183-194.
55. Vagedes, P., B. Rabenstein, J. Aqvist, J. Marelius, and E.W. Knapp, The deacylation step of acetylcholinesterase: Computer simulation studies. *Journal of the American Chemical Society*, **2000**. 122(49): p. 12254-12262.
56. Nemukhin, A.V., S.V. Lushchekina, A.V. Bochenkova, A.A. Golubeva, and S.D. Varfolomeev, Characterization of a complete cycle of acetylcholinesterase catalysis by ab initio QM/MM modeling. *Journal of Molecular Modeling*, **2008**. 14(5): p. 409-416.
57. Humphrey, W., A. Dalke, and K. Schulten, VMD-Visual Molecular Dynamics. J. Molec. *Graphics*, **1996**. 14(1): p. 33-38.
58. Stone, J., Efficient Library for Parallel Ray Tracing and Animation, in Computer Science Department1998, University of Missouri-Rolla: Rolla.
59. Papadopoulos, J.S. and R. Agarwala, COBALT: constraint-based alignment tool for multiple protein sequences. *Bioinformatics*, **2007**. 23(9): p. 1073-1079.
60. Sanner, M.F., A.J. Olson, and J.C. Spehner, Reduced surface: An efficient way to compute molecular surfaces. *Biopolymers*, **1996**. 38(3): p. 305-320.